Available online at www.sciencedirect.com
ScienceDirect
Ceramics International 36 (2010) 943–946
CERAMICS INTERNATIONAL
www.elsevier.com/locate/ceramint

Transmission electron microscopy characterization of spark plasma sintered ZrB_2 ceramic

Takashi Mizuguchi [a], Shuqi Guo [a,*], Yutaka Kagawa [a,b]

[a] Hybrid Materials Center, National Institute for Materials Science, 1-2-1 Sengen, Tsukuba, Ibaraki 305-0047, Japan
[b] Research Center for Advanced Science and Technology, The University of Tokyo, 4-6-1 Komaba, Meguro, Tokyo 153-8904, Japan

Received 24 August 2009; received in revised form 23 September 2009; accepted 21 October 2009
Available online 20 November 2009

Abstract

Microstructures of ZrB_2 ceramics consolidated by hot-pressing and spark plasma sintering were investigated by transmission electron microscopy (TEM), combining energy dispersive X-ray spectroscopy (EDX). The microstructures of both ceramics were compared. Amount of impurities was lower for ZrB_2 consolidated by spark plasma sintering than for hot-pressed ZrB_2. In particular, oxygen impurity was not detected even at the grain-boundaries in ZrB_2 consolidated by spark plasma sintering. The cleaning effect generated on the powder surfaces during spark plasma sintering cycle was displayed. In addition, dislocations were present only in the spark plasma sintered ZrB_2 ceramic, as a result of localized high stresses.

Keywords: Zirconium diboride; Microstructure; Spark plasma sintering; Transmission electron microscopy

1. Introduction

Spark plasma sintering (SPS) is one of the most recent advanced processing techniques developed for densifying ceramic materials [1,2]. Although SPS is similar to hot-pressing (HP), in place of indirect heating, the applied electrical field heats the die and the powder compact. The SPS makes it possible to sinter body material at lower temperatures and in a shorter time than in conventional hot-press sintering. Previous studies [3–5] on several carbide, nitride, and oxide ceramics have also shown that the SPS produced almost full density at a lower temperature, with a considerable shorter sintering time (within minutes), compared to hot-pressing, thereby retaining fine and homogeneous microstructure. Recent studies have shown that SPS enhanced densification and the refined microstructure can be achieved in very short processing cycles for ZrB_2-based ceramics [6–8]. For example, ZrB_2–ZrC–SiC compositions could be sintered to fully dense compacts with fine and homogenous microstructure at 1950 °C and 30 MPa for 2 min [7], by using the SPS technique. Full densified pure ZrB_2 could be achieved at 1900 °C and 50 MPa for 3 min [8] by SPS as well. For comparison, the ZrB_2 produced by HP achieved a relative density of ~91% even at 2000 °C and 30 MPa for 60 min [9]. Hence, the SPS process could be used to enhance densification of poorly sinterable ceramics, by simultaneously applying a uniaxial load and a direct or pulsed electric current to a powder compact.

It has been recognized that the SPS enhances densification and improves sinterability of ZrB_2-based ceramics. However, the densification enhancing mechanism – mainly whether or how an electric discharge is involved in accelerating the densification and grain growth – is still the subject of intense debate. Four factors that contribute to the fast densification process can be discerned: (i) an efficient heat transfer; (ii) the use of comparatively high pressure; (iii) the presence of an electrical field (use of DC pulses); and (iv) the presence of local spark discharges generated between the powder particles under high-energy electrical pulses. Presumably, the presence of discharge cleans the powder surfaces from adsorbed species, promoting their activation [1]. The presence of cleaned and activated surfaces is expected to enhance the grain boundary diffusion, therefore densification. Obviously, it is important to identify whether the cleaning effect is present or absent during the SPS cycle. It could be expected the impurities at the grains

* Corresponding author. Tel.: +81 029 859 2223; fax: +81 029 859 2401.
E-mail address: GUO.Shuqi@nims.go.jp (S. Guo).

0272-8842/$36.00
doi:10.1016/j.ceramint.2009.10.025

boundary of the sintered ZrB_2 compacts to be considerably lower for the SPS samples than for the HP ones when the cleaning effect was present on the powder surfaces. In this study, the grain-boundary microstructures of ZrB_2 ceramics produced by SPS and HP were characterized by transmission electron microscopy. Also, the chemical compositional analysis of grain-boundaries for the both ZrB_2 ceramics was carried out by an energy dispersive X-ray spectroscopy (EDX) under the TEM observations.

2. Experimental

Commercially available ZrB_2 powder (Grade F, Japan New Metals Co., Ltd., Tokyo) was used in this study. The particle size of the powder is in the range of 1.5–2.5 μm, with an average grain diameter of 2.1 μm. The elemental impurities are (wt.%): O 1.06, C 0.27, N 0.19, and a few of Cr, Fe and Hf. In order to eliminate large ZrB_2 agglomerates, the starting ZrB_2 powder was homogenized by ball milling in silicon carbide media using ethanol as a solvent for 24 h and the resulting slurry was then dried. The powder was put into a graphite die lines with graphite foil and densified using plasma spark sintering (SPS-1030, Sumitomo Coal Mining Co. Ltd., Tokyo, Japan). The sintering was performed at 1900 °C and 50 MPa for 3 min in vacuum ($\sim 6 \times 10^{-2}$ Pa), with heating rate of ~200 °C/min. The load was removed when the die temperature dropped to below 1000 °C, with the cooling rate of ~600 °C/min. In addition, the hot-pressed ZrB_2 samples were prepared for comparison. The hot-pressing was conducted at 2000 °C for 60 min under an external pressure of 30 MPa in vacuum. The detailed SPS and HP processes were reported elsewhere [8,9]. The SPS and HP sintering conditions, relative density, and grain diameter of the resulting specimens were summarized in Table 1.

The crystalline structure of the ZrB_2 ceramics consolidated by HP and SPS was identified by X-ray diffraction (XRD; RINT2500, Rigaku Co. Ltd., Tokyo, Japan) with Cu Kα and an accelerating voltage of 40 kV and a current of 200 mA. Thin specimens for TEM observations were mechanically ground to a thickness of ~80 μm, then dimpling to a thickness of ~20 μm in the center of the disks and additional Ar^+-ion beam thinning at accelerating voltage of 4 kV. The microstructures of both ceramics were investigated by transmission electron microscopy (JEOL JEM-2010F) operated at 200 kV. Energy dispersive X-ray spectroscopy (EDX) analysis was also done using a NORAN 663D spectrometer during TEM observation in order to determine impurities inside the grains and at the grain-boundaries for the SPS and HP sintered ZrB_2 ceramics.

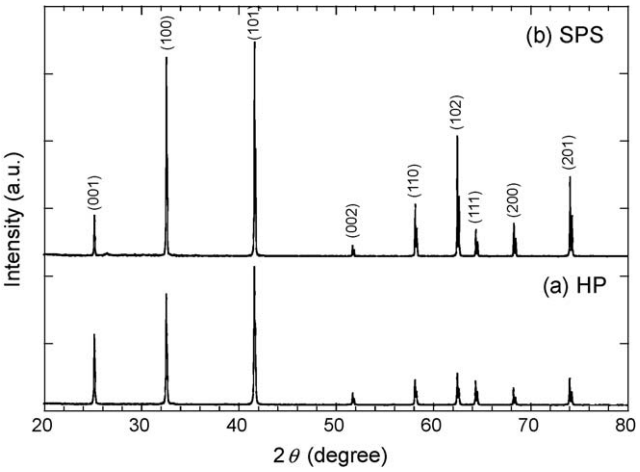

Fig. 1. X-ray diffraction patterns of the ZrB_2 ceramics consolidated by (a) HP, and (b) SPS.

3. Results and discussion

In Fig. 1, the X-ray diffraction patterns for the both ZrB_2 ceramics consolidated by HP and SPS are presented. Only hexagonal ZrB_2 phase was detected in both sintered materials, whereas the intergranular secondary phase was not detected for both materials. In Fig. 2, a bright-field TEM image of the hot-pressed ZrB_2 is presented. Most of the grains showed equiaxed shape with average grain diameter of 4.5 μm. However, several grains had preferentially grown to an elongated rod with an average aspect ratio of ~1.8. The EDX spectra of the inside of ZrB_2 grain and the grain boundary (marked A and B in Fig. 2(a)) are shown in Fig. 2(b) and (c), respectively. Characteristic X-rays of B, O, Cu, Zr and Hf elements were present inside the ZrB_2 grain (Fig. 2(b)). *Note that the Cu signals are from background generated from Cu mesh*. O and Hf result from the impurities of the starting ZrB_2 powders and they are also present inside the ZrB_2 grains. On the other hand, Fe and Cr are present at the grain-boundaries as well (Fig. 2(c)). Also, the amounts of the impurities are significantly higher at the grain-boundaries than inside the ZrB_2 grains. Impurities presence inhibited the densification of the ZrB_2 ceramic and promoted grain growth during the hot-pressing sintering.

In Fig. 3, a bright-field TEM image of the ZrB_2 ceramic consolidated by SPS is presented. The ZrB_2 ceramic consolidated by SPS showed fine and homogenous microstructure which consisted of almost equiaxed grains, compared to the hot-pressed ZrB_2 ceramic (Fig. 2(a)). The average grain size was approximately 2.7 μm, i.e. smaller than for hot-pressed ZrB_2 (Table 1). This is attributed to a lower sintering

Table 1
Sintering conditions, densities, and average grain size of the ZrB_2 ceramics consolidated by HP and SPS.

Sintering route	Consolidated conditions	Theoretical density (g/cm^3)	Measured density (g/cm^3)	Relative density (%TD)	Average grain size of ZrB_2	
					d (μm)	Aspect ratio
Hot-pressing	2000 °C/60 min/30 MPa/vacuum	6.09	5.51	90.4	4.5	1.8
Spark plasma sintering	1900 °C/3 min/50 MPa/vacuum	6.09	5.94	97.6	2.7	1.2

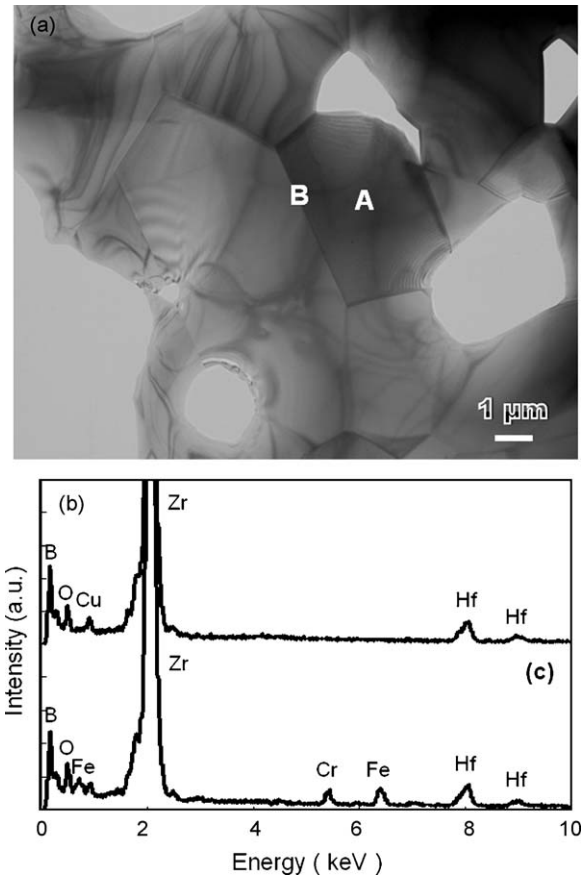

Fig. 2. (a) TEM bright-field image, and EDX spectra obtained (b) inside the ZrB_2 grain (marked A in (a)), and (c) at the grain-boundary (marked B in (a)) for the ZrB_2 ceramics consolidated by HP.

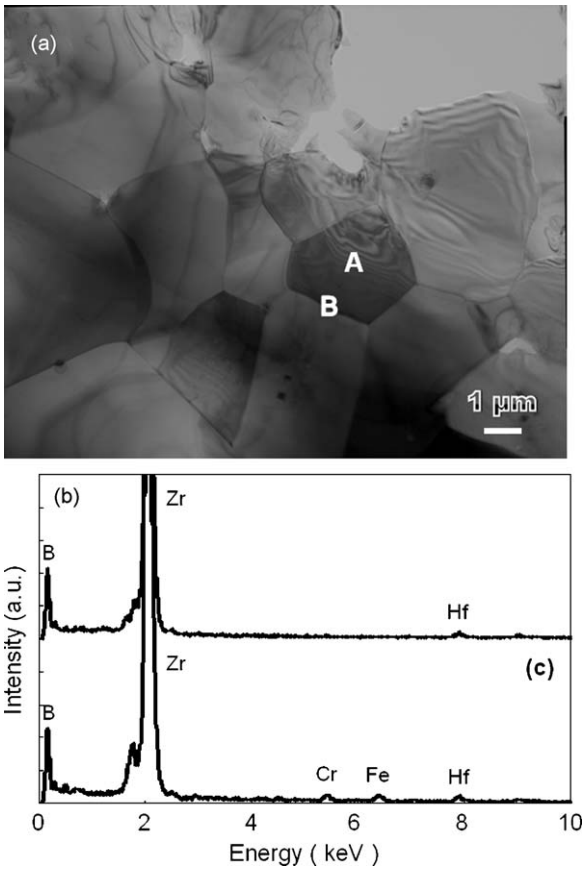

Fig. 3. (a) TEM bright-field image, and EDX spectra obtained (b) inside the ZrB_2 grain (marked A in (a)), and (c) at the grain-boundary (marked B in (a)) for the ZrB_2 ceramics consolidated by SPS.

temperature and much shorter sintering time for SPS than for HP (Table 1). The EDX spectra of the inside of ZrB_2 grain and the grain boundary (marked A and B in Fig. 3(a)) are shown in Fig. 3(b) and (c), respectively. Only Hf impurity is present inside the ZrB_2 grains, whereas Cr, Hf and Fe are detected at the grain-boundaries. Furthermore, the intensities of the Hf peak detected inside the grains are almost the same as at the grain-boundaries. In addition, the intensities of these impurities are considerably lower for the SPS specimens than for the HP ones (Fig. 2(b) and (c)). In particular, oxygen was not detected either inside the ZrB_2 grains or at the grain-boundaries for the SPS specimen. Obviously, the absence of oxygen and the reduced amount of Hr, Cr and Fe impurities are closely linked to the high-energy electrical pulse during the SPS cycle; indeed, oxygen was present inside the grains and at the grain-boundaries for the hot-pressed ZrB_2 ceramic (Fig. 2(b) and (c)), demonstrating that cleaning of ZrB_2 particles surfaces results from the SPS cycle. Presumably, the presence of oxygen within the ZrB_2 grains for the hot-pressed ZrB_2 ceramic is probably a result of inward diffusion of oxygen impurities (B_2O_3 and ZrO_2) present on the ZrB_2 powder surfaces during hot-pressing sintering. It should be believable that this cleaning effect results from the spark discharge generated between the powder particles under a high-energy electrical pulse during the SPS cycle.

Oxygen impurities (B_2O_3 and ZrO_2) present on the starting powder surfaces have been shown to inhibit densification and to promote grain growth in non-oxide ceramic systems [10,11]. A study [11] on TiB_2 suggested that the total oxygen content must be less than 0.5 wt.% to achieve full density. Thus, it is important to reduce the amount of oxygen for enhancing densification and improving sinterability. Previous studies [12–14] on ZrB_2 ceramics with nitride additives, e.g. Si_3N_4, AlN, HfN or ZrN, showed their suitability is effective additives for improving sinterability or/and enhancing densification of ZrB_2. The main reason for incorporating nitrides as additives is the propensity of nitrides to consume the oxygen-bearing species on the diboride powder surfaces. The reduction of oxygen results in higher boron activity, which is one of the conditions favouring lattice diffusion and, therefore, densification [11]. Thus, the fine and homogenous microstructure as well as the lower sintering temperature required for SPS specimens is attributed to oxygen absence as well as other impurities reduction on the ZrB_2 powder surfaces during the SPS cycle. This cleaning effect occurring at the initial stage of sintering results in cleaned and active surfaces of ZrB_2 particles, a factor that is expected to enhance the grain boundary diffusion, and thus densification.

Moreover, some dislocations were observed in the ZrB_2 ceramics consolidated by SPS (Fig. 4). These dislocations

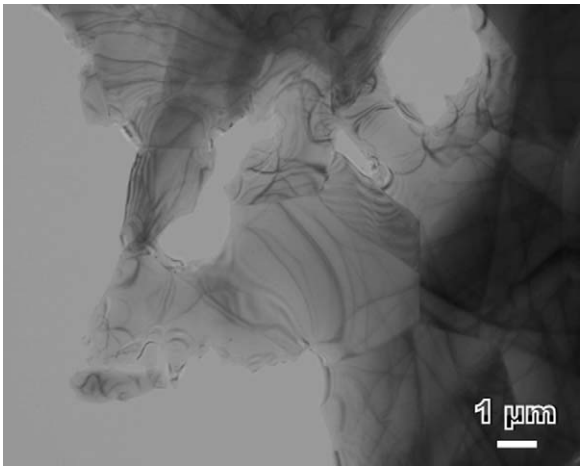

Fig. 4. TEM bright-field image of the ZrB_2 ceramics consolidated by SPS, showing dislocations presence in the ZrB_2 grains.

originated from the ZrB_2 grains boundaries and cross the grains, suggesting the ZrB_2 grains to be deformed during the SPS cycle. However, dislocations were not observed in the hot-pressed ZrB_2 ceramics (Fig. 2(a)). A study [15] in ZrB_2–ZrC composite consolidated by SPS at 1800 °C and 50 MPa for 5 min showed well-ordered dislocations in the ZrB_2 grains, whose presence was attributed to a localized high stresses originated from the sharp thermal gradient during the SPS cycle. Similar effect may be effective in fast cooling cycle (cooling rate: ∼600 °C/min) utilized in this study.

4. Conclusions

The microstructure of hot-pressed ZrB_2 ceramics consisted of equiaxed grains and a few of elongated grains. The microstructure of spark plasma sintered ZrB_2 ceramic consisted of equiaxed grains. The average diameter of grains was smaller for the spark plasma sintered ZrB_2 ceramics than for the hot-pressed ones. This was attributed to the lower sintering temperature and very shorter sintering time for SPS, compared to HP. O and Hf were present inside the ZrB_2 grains and at the grain-boundaries of hot-pressed ZrB_2, whereas Cr and Fe were found only at the grain-boundaries. For the spark plasma sintered ZrB_2, on the other hand, oxygen was not detected neither inside ZrB_2 grains nor at the grain-boundaries. A few Cr, Fe and Hf were present at the grain-boundaries. Oxygen absence and the low impurity content at the grain-boundaries were attributed to the cleaning of ZrB_2 particles surfaces during the SPS cycle, resulting from the spark discharge generated between ZrB_2 powder particles under high-energy electrical pulses. In addition, dislocations were present only in the ZrB_2 ceramics consolidated by SPS, whose presence was associated to localized high stresses which originated from the sharp thermal gradient during cooling.

References

[1] M. Tokida, Trends in advanced spark plasma sintering system and technology, J. Soc. Powder Technol. Jpn. 30 (11) (1993) 790–804.
[2] M. Nygren, Z. Shen, On the preparation of bio-, nano- and structural ceramics and composites by spark plasma sintering, Solid State Sci. 5 (2003) 125–131.
[3] F Guillard, A. Allemand, J.D. Lulewicz, J. Galy, Densification of SiC by SPS—effects of times, temperature and pressure, J. Eur. Ceram. Soc. 27 (2007) 2725–2728.
[4] K.A. Khor, K.H. Cheng, L.G. Yu, F. Boey, Thermal conductivity and dielectric constant of spark plasma sintered aluminum nitride, Mater. Sci. Eng. A 347 (2003) 300–305.
[5] Z. Shen, M. Johnsson, Z. Zhao, M. Nygren, Spark plasma sintering of alumina, J. Am. Ceram. Soc. 85 (8) (2002) 1921–1927.
[6] A. Bellosi, F. Monteverde, D. Sciti, Fast densification of ultra-high-temperature ceramics by spark plasma sintering, Int. J. Appl. Ceram. Technol. 3 (1) (2006) 32–40.
[7] S.Q. Guo, Y. Kagawa, T. Nishimura, D. Chung, J.-M. Yang, Mechanical and physical behavior of spark plasma sintered ZrC–ZrB_2–SiC multiphase composites, J. Eur. Ceram. Soc. 28 (2008) 1279–1285.
[8] S.Q. Guo, T. Nishimura, Y. Kagawa, J.-M. Yang, Spark plasma sintering of zirconium diborides, J. Am. Ceram. Soc. 91 (9) (2008) 2848–2855.
[9] S.Q. Guo, J.-M. Yang, H. Tanaka, Y. Kagawa, Effect of thermal exposure on strength of ZrB_2-based composites with nano-sized SiC particles, Compos. Sci. Technol. 68 (14) (2008) 3033–3040.
[10] S.Q. Guo, Densification of ZrB_2-based composites and their mechanical and physical properties: a review, J. Eur. Ceram. Soc. 29 (2009) 995–1011.
[11] S. Baik, P.F. Becher, Effect of oxygen contamination on densification of TiB_2, J. Am. Ceram. Soc. 70 (8) (1987) 527–530.
[12] F. Monteverde, A. Bellosi, Effect of the addition of silicon nitride on sintering behavior and microstructure of zirconium diboride, Scripta Mater. 46 (2002) 223–228.
[13] F. Monteverde, A. Bellosi, Beneficial effects of AlN as sintering aid on microstructure and mechanical properties of hot-pressed ZrB_2, Adv. Eng. Mater. 5 (7) (2003) 508–512.
[14] F. Monteverde, A. Bellosi, Efficacy of HfN as sintering aid in the manufacture of ultra-high-temperature metal diborides-matrix ceramics, J. Mater. Res. 19 (12) (2004) 3576–3585.
[15] K.H. Kim, K.B. Shim, Effect of lanthanum on the fabrication of ZrB_2–ZrC composites by spark plasma sintering, Mater. Charact. 50 (2003) 31–37.